BEIJING 1988

THE INTERNATIONAL SYMPOSIUM
ON HYDRAULICS FOR HIGH DAMS

Hydraulics and design of spillway aerators for cavitation prevention in high speed flows

Dr.-Ing. Hans-Peter Koschitzky and Prof. Dr. Helmut Kobus
Institut für Wasserbau, Universität Stuttgart
Federal Republic of Germany

Summary
The controlling factors for spillway aeration are discussed in view of their relevance to the design of aerators. The air entrainment results from the interaction of the water flow and the air flow in the supply system. An empirical two dimensional air entrainment function for various aerator geometries is presented. The subatmospheric pressure distribution in the aerator is calculated by an iterative method. The combination of both yields the total air entrainment rate. The air entrainment leads to an increase of the water flow velocity.

1. INTRODUCTION

In high velocity flows such as in concrete spillways or bottom outlets, cavitation can lead to heavy damages within a short time. Cavitation damage can be prevented by means of flow aeration. Prototype experiences with well working aeration systems confirm the reliability of this method. *Minor (1987)* describes a bottom outlet with only one aerator for a length of 400 m, running one year with flow velocities of about 40 m/s without any cavitation damages. However, it has to be noted that some plants with aeration systems are working well in view of cavitation preventation, but show excessive air entrainment and hence unexpected flow effects *(for example Minor, 1987)*. Most noteably the entrained air leads to an acceleration of the flow *(Koschitzky, 1987, and 1988)*. This effect has to be considered in the design of the energy dissipator.

A spillway aeration device consists of two main components *(see fig. 1)* : an air supply system and a bottom device with a surface discontinuity at which the air is entrained by the water flow.

2. CONTROLLING FACTORS FOR AIR ENTRAINMENT

With regard to the process of air entrainment, four different limiting conditions can be distinguished *(Kobus 1984, 1985)*. The relevant controlling factors are discussed in view of spillway aeration devices:

Inception limit
For a given flow configuration, the flow conditions must be such as to generate a sufficiently large disturbance for air entrainment to occur. The inception limit depends strongly upon the fluid properties and characterizes the condition that inertial reactions become large enough to overcome the resisting forces due to viscosity and surface tension. In prototype spillway flows, this condition is always given and hence this limit is no controlling factor.

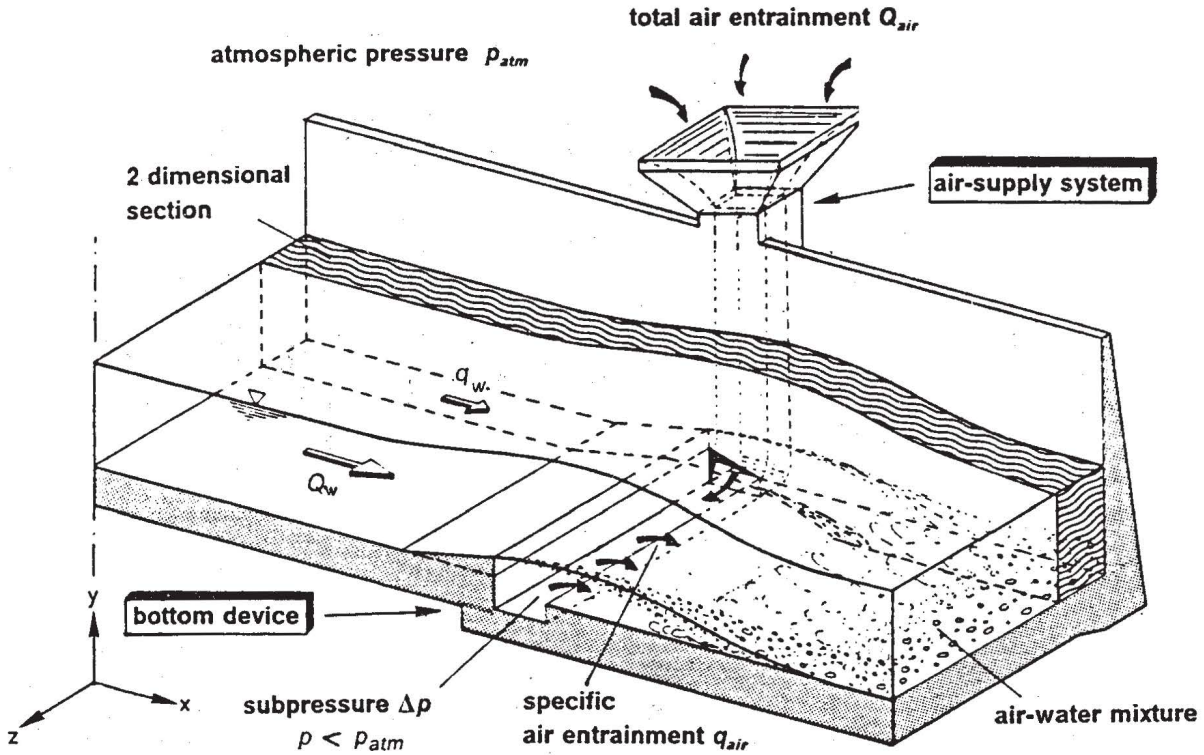

Fig. 1: *Sketch of a typical spillway aerator*

Entrainment limit

The conditions of the approach flow govern the entrainment limit. These conditions are quantified by the Froude number Fr. Depending upon the boundary geometry, a critical value of Fr must be exceeded for air entrainment to occur. For higher Froude numbers, the approach flow provides the driving mechanism for the air entrainment. In high velocity spillway flows, the value of Fr usually exceeds the critical value.

Air supply limit

At aerators, air is entrained from a limited enclosed air space, which is connected to the atmosphere by an air supply system *(Fig. 1)*. The supply of air to the point of entrainment into the water requires an air flow through the supply system. This flow necessarily results in a pressure difference between the atmosphere and the cavity below the nappe. The subatmospheric pressure at the location of air entrainment depends upon the air entrainment rate and the losses in the air supply system. As it is sketched in *Fig. 2*, the pressure difference is a maximum when the air duct is closed (i. e. zero air entrainment) and decreases to zero for unlimited air supply (maximum air entrainment). Depending upon the head loss characteristics of the air supply system, there results an operating point characterizing the resulting air supply rate and the corresponding pressure difference. This means the supply system is limiting the air entrainment.

Moreover, the air flow in the bottom installation leads to a pressure distribution in the air cavity across to the water flow. Therefore, the operating point and hence the specific air entrainment is not constant across the spillway. The pressure distribution over the spillway width has to be considered in the evaluation of the total air entrainment rate.

Transport limit

The transport capacity of the flow is governed by the downstream flow conditions. It depends upon the flow velocity and turbulence as determined by the wall shear stresses *(Wood, 1983)*. The transport capacity determines the downstream length over which an aerator is effective and hence the spacing of the aerator devices. It usually is not limiting the air entrainment at the aerator, except in cases in which the water depth is very small compared to the water jet length, or in cases of excess air in the approach flow.

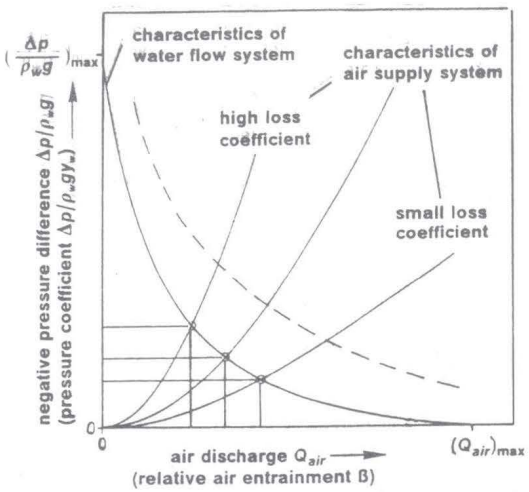

Fig. 2: *Characteristics of the water flow and the air supply system*

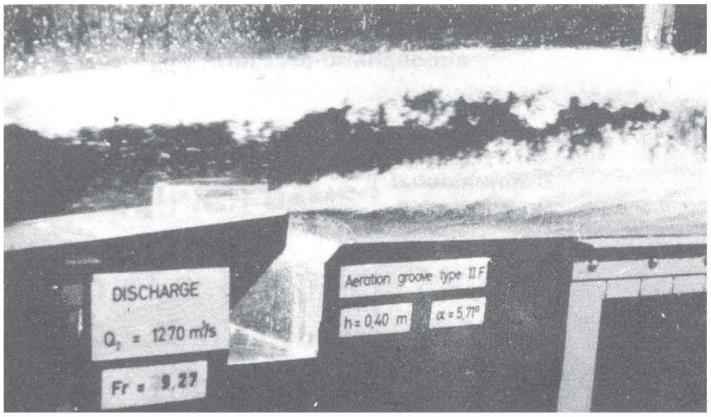

Fig. 3: *Air entrainment at the interface of the water jet and the air in the cavity (Flow velocity v_w = 13 m/s; water depth y_w = 200 mm)*

3. AIR ENTRAINMENT MECHANISMS

The physics of the air entrainment mechanism at aerators are not well understood. However several principal reflections and ideas of the process exist *(Koschitzky, 1987; Ervine, Falvey, 1987)*. Photos *(Fig. 3)* and high-speed movies showed *(Koschitzky, Barczewski, 1987)* that the air entrainment occurs along the jet length, beginning at the end of the ramp. This means that the air entrainment can be regarded as a shear phenomenon at the interface of the water jet and the air in the cavity. Air is entrained by vortices at the interface, which result from the sudden pressure drop at the ramp edge, from the corresponding change in velocity distribution, from the turbulent fluctuations in the approach flow, and from the upstream pressure disturbance due to the ramp geometry.

It is not clear which of these effects is dominating, but model investigations confirm that the air entrainment is related to the length of the air-water interface of the cavity, which for a given aerator geometry can be expressed by the Froude number of the flow.

With regard to the influence of the approach flow turbulence intensity, model tests *(Koschitzky, 1987)* showed that a marked increase of the surface roughness on the aerator ramp results in a corresponding increase of the air entrainment by 20% to 30 %.

4. TWO-DIMENSIONAL AIR ENTRAINMENT FUNCTION

A dimensional analysis *(Kobus, 1984; Koschitzky, 1987)* yields the following relationship for the specific air entrainment rate β:

$$\beta = \frac{q_{air}}{q_w} = f(Fr;\ \Delta p/\rho_w g y_w;\ \textbf{aerator geometry}) \qquad [1]$$

In a systematic experimental investigation *(Koschitzky, 1987)*, two typical types of aerators were investigated: a ramp (type I) for the use in steep slopes, and a groove with ramp (type II) for small slopes. A sectional model and a full width model were used. The scale between the models was 1:3.75. The main technical data of both models are described in *(Koschitzky et al. 1984 and Koschitzky, 1987)*. In the full width model, it was possible to vary the spillway width in order to investigate 3-dimensional effects in comparison to the 2-dimensional sectional model. In the large sectional model a blower was connected to the air supply system in order to investigate the effect of pressure variation in the cavity below the nappe, including the case of atmospheric pressure ($\Delta p = 0$).

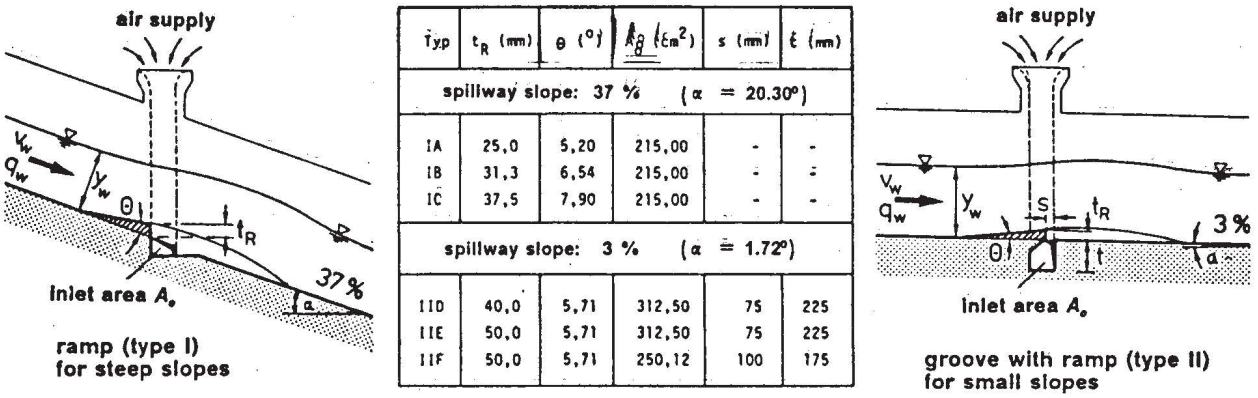

Typ	t_R (mm)	θ (°)	A_e (cm²)	s (mm)	t (mm)
spillway slope: 37 % (α = 20.30°)					
IA	25,0	5,20	215,00	-	-
IB	31,3	6,54	215,00	-	-
IC	37,5	7,90	215,00	-	-
spillway slope: 3 % (α = 1.72°)					
IID	40,0	5,71	312,50	75	225
IIE	50,0	5,71	312,50	75	225
IIF	50,0	5,71	250,12	100	175

Fig. 4: *Investigated geometries of the two aerator types*

The measurements show that for a the case of no subpressure ($\Delta p = 0$) and for a given pressure parameter ($\Delta p/\rho_w g y_w$ *const.*) the entrainment rate β is a unique function of the flow Froude number Fr *(Fig. 5)*. All these functions tend towards ($\beta = 0$) at approximately the same Froude number which is indicated as Fr_{crit}. This so called critical Froude number Fr_{crit} has a constant value for a given aerator geometry, but of course varies with the geometry of the aerator. *Rutschmann (1988)* has pointed out, that at smaller Froude numbers one still can observe air entrainment, with very small values of β. For design purposes, however, this effect is not significant. The two-dimensional air entrainment rate can therefore be described by an empirical function of the general form:

$$\beta = C1(Fr - Fr_{crit})^{C3}\left(1 - C2\left(\frac{\Delta p}{\rho_w g y_w}\right)\right) \qquad [2]$$

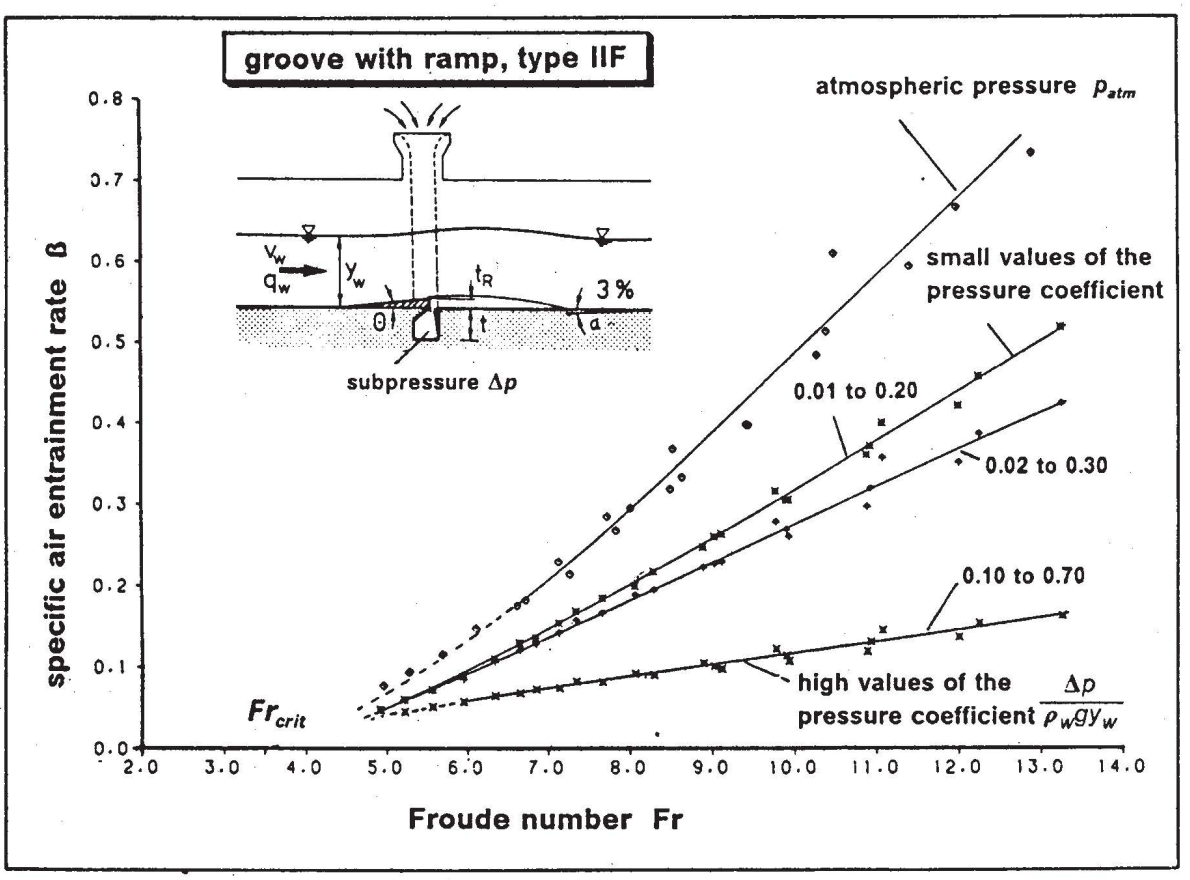

Fig. 5: *Specific air entrainment rate as a function of the Froude number and the pressure coefficient*

For all investigated geometries including the published data from *Tan (1984)* and *Low (1986)* and recent measurements by *Rutschmann (1988)* for other geometries, it can be observed that the exponent C3 only varies in a narrow range about the value 1.5. Therefore the entrainment function can be presented in the form:

$$\beta = C1(Fr - Fr_{crit})^{1.5}\left(1 - C2\left(\frac{\Delta p}{\rho_w g y_w}\right)\right) \qquad [3]$$

A comparison of measured and calculated entrainment rates is given in *Fig. 6* for the geometries of *Fig. 4* and in *Fig. 7* for the geometries of *Rutschmann (1988)*. The values of the coefficients, which depend upon the aerator geometry, are summarized in *Fig. 8*.

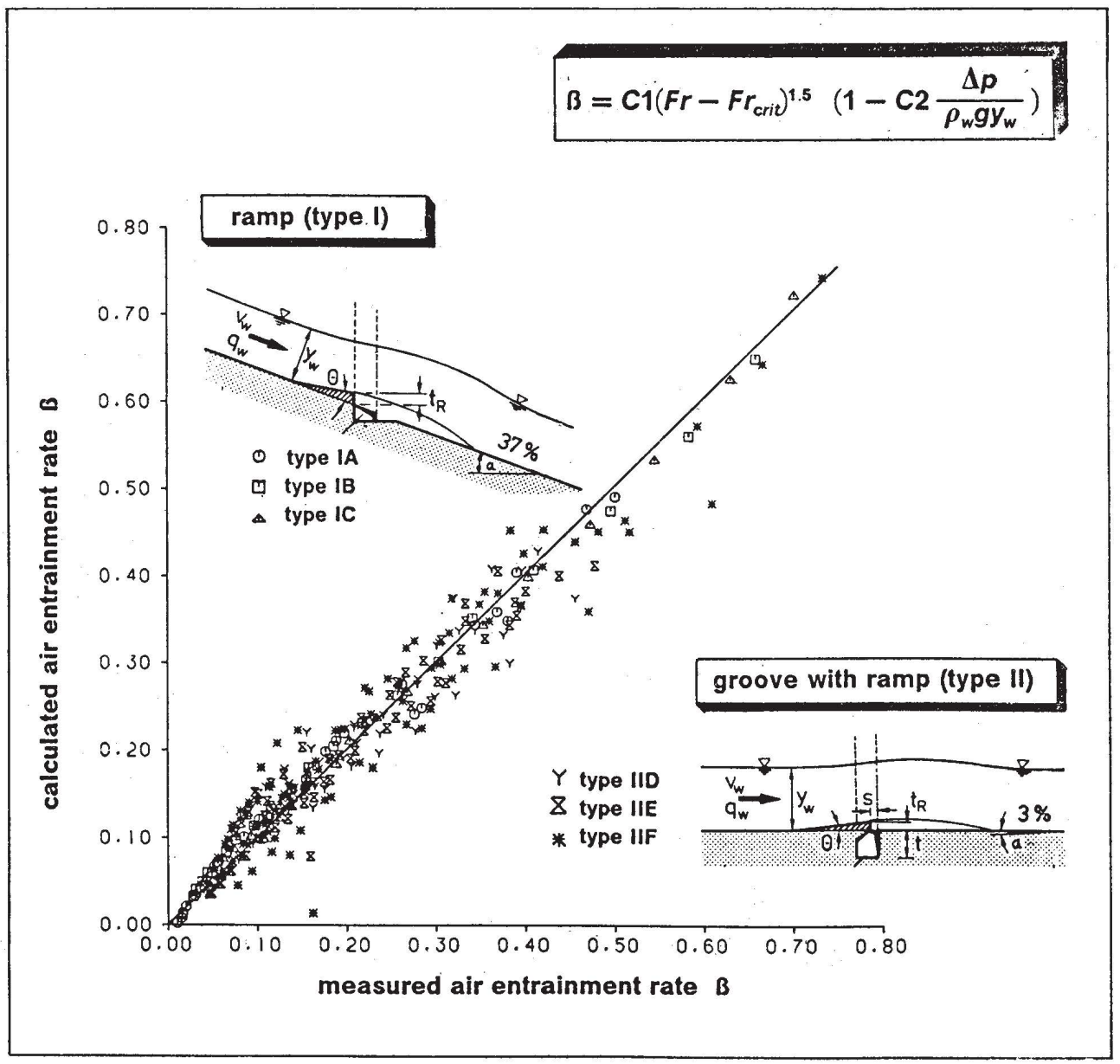

Fig. 6: *Comparison of the measured and calculated air entrainment rates for all investigated geometries of type I and II*

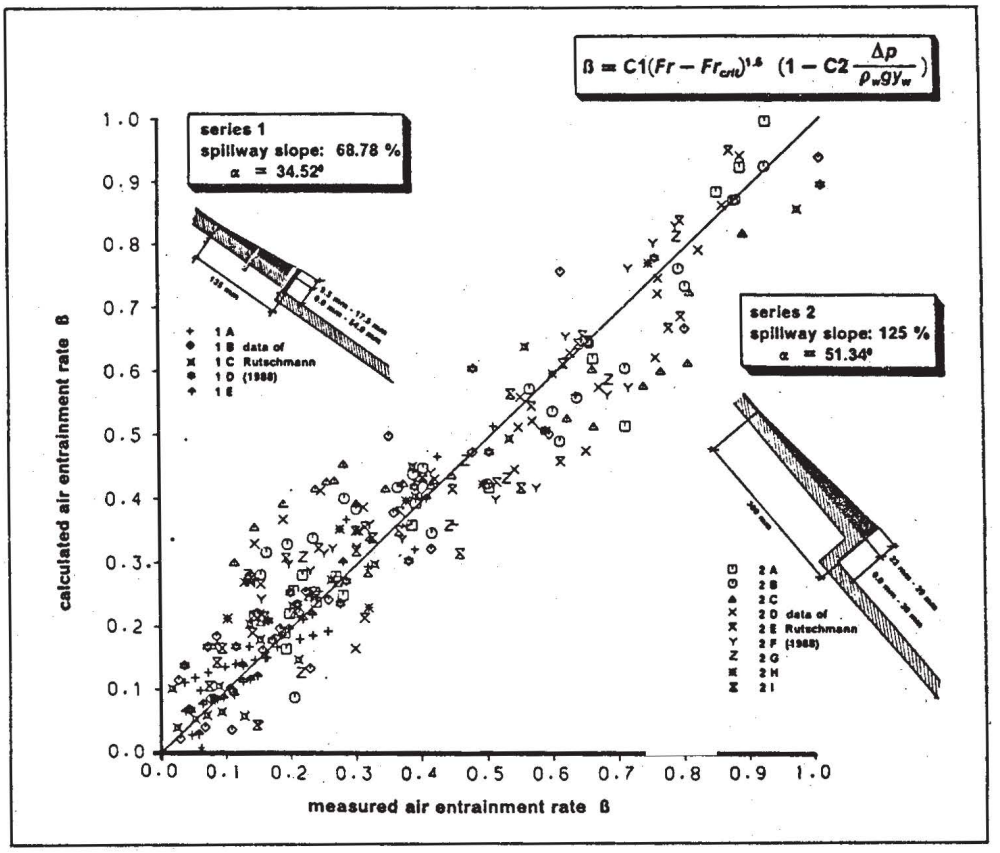

Fig. 7: *Comparison of the measured and calculated air entrainment rate for Rutschmann's (1988) geometries*

specific air entrainment function $ß = C1(Fr - Fr_{crit})^{1.5} \left(1 - C2 \frac{\Delta p}{\rho_w g y_w}\right)$

aerator type	α	θ	sketch	C1	C2	Fr_{crit}	data in
ramp type IA,B,C	20.3°	5.2°-7.9°	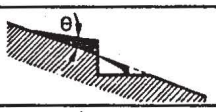	0.022 ±0.002	0.03 ±0.002	3.5 ±0.7	Koschitzky (1987)
groove with ramp type IID,E,F	1.71°	5.71°		0.02 ±0.005	1.25 ±0.25	3.7 ±0.2	Koschitzky (1987)
ramp	14.5°	7.1°		0.040 ±0.015	1.05 ±0.02	3.0 ±0.5	Tan (1984)
series 1 1A 1D ramp 1E	34.52°	4.0°-7.6°	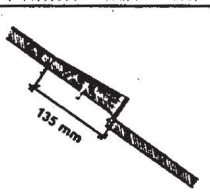	0.035 ±0.01	1.050 ±0.15	4.0	Rutschmann (1988)
1B ramp with step 1C	34.52°	5.71°		0.045 ±0.005	2.250 ±0.15	4.0	
series 2 2A 2B ramp with step 2C	51.34°	7.4069°	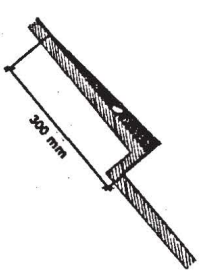	0.100 ±0.040	5.00 ±1.00	3.0 ±1.0	
2D 2E ramp with step 2F	51.34°	5.71°		0.075 ±0.015	3.60 ±0.7	3.0	Rutschmann (1988)
2G 2H ramp with step 2I	51.34°	4.38°		0.056 ±0.005	2.65 ±0.45	2.5	

Fig. 8: *Coefficients of the air entrainment function for various aerator geometries*

5. TOTAL AIR ENTRAINMENT

As shown in *Fig. 9*, the air flow in the aerator can be divided in two parts: the flow in the air duct and the flow in the bottom installation. The pressure difference Δp_0 between the intake of the air duct and the inlet area A_0 in the spillway side wall can be calculated from the energy losses in the air duct system, which are composed of the friction losses and the various local losses. For the usual dimensions of aerators and supply systems friction effects can be neclected compared to the local losses. These losses can be estimated from *Koschitzky (1987)* or *Rutschmann (1987, 1988)*. Summarizing all local losses in one total loss coefficient ξ_0 the subpressure Δp_0 at the inlet section A_0 can be expressed as:

$$\Delta p_0 = (\xi_0 + 1)\frac{\rho_{air} v_{air,0}^2}{2} \qquad [4]$$

The air flow in the bottom installation leads to a sort of manifold flow. Across the spillway, the flow rate decreases from the value of the total air entrainment Q_{air} to zero. This leads to a distribution of the subpressure in the cavity below the nappe as sketched in *Fig. 9*. Model investigations in the full width model with variable spillway chute width, confirmed this pressure distribution *(Fig. 10)*. They showed furthermore that the flow cross section can be assumed constant across the width and equal to the value of the inlet area A_0 , and that the head losses of the air cross flow can be neglected. This means that the subpressure Δp_B at the centerline of the spillway is equal to the headlosses in the duct system:

$$\Delta p_B = \xi_0 \left(\frac{\rho_{air} v_{air,0}^2}{2}\right) = \Delta p_0 - \frac{\rho_{air} v_{air,0}^2}{2} \qquad [5]$$

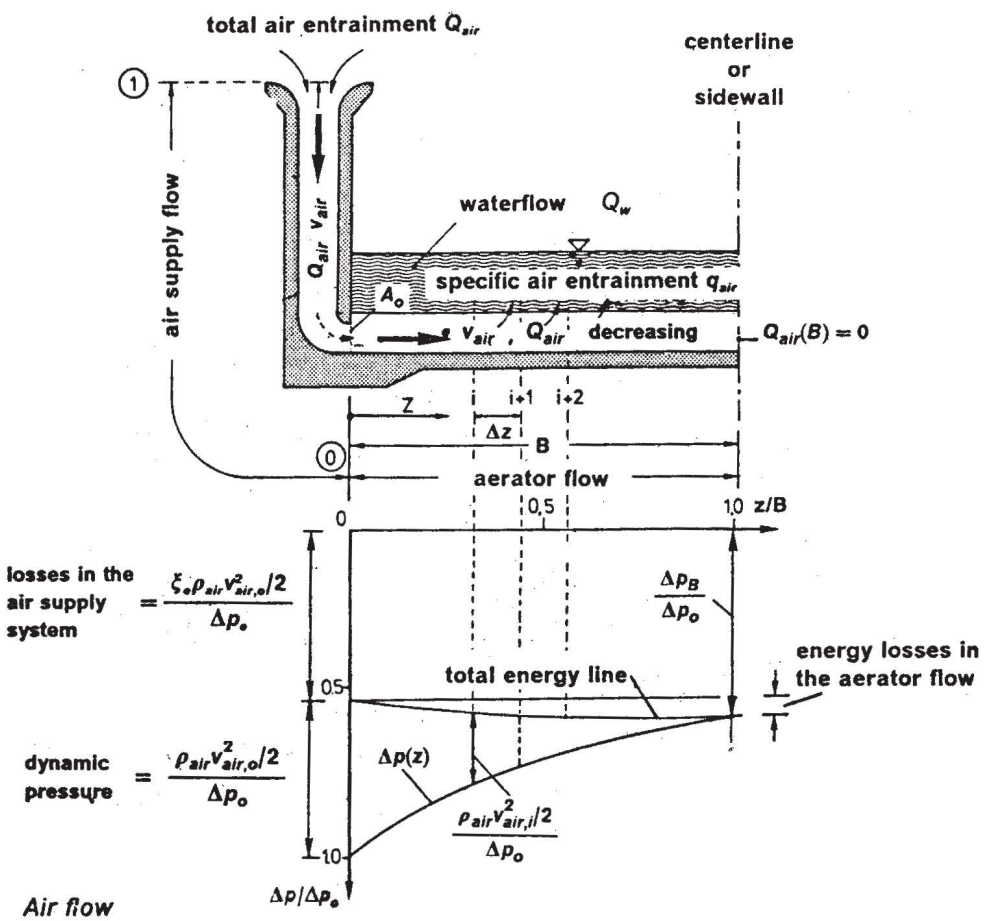

Fig. 9: *Air flow*

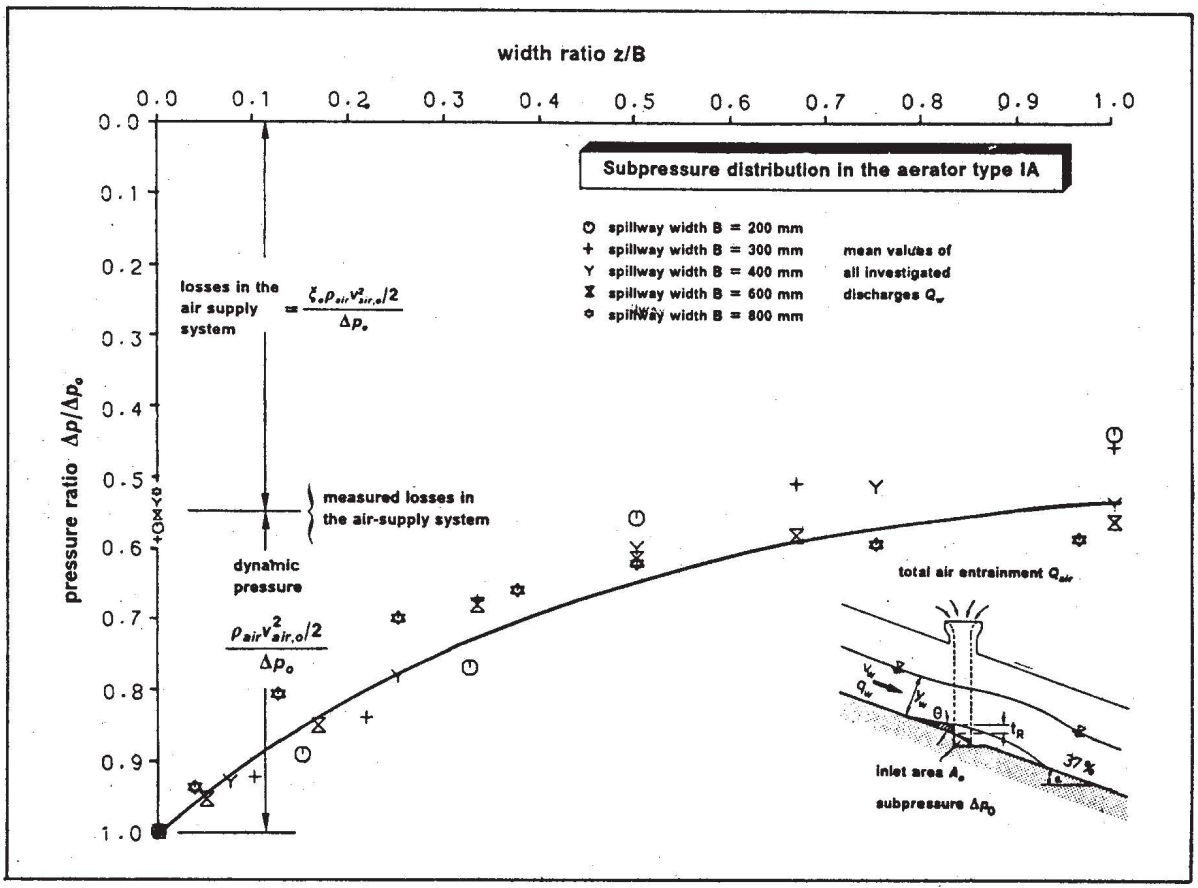

Fig. 10: *Measured pressure distribution in the aerator of type I for various spillway widths*

Knowing the two-dimensional air entrainment function (Eq. 3), the air flow and the total air entrainment Q_{air} can be calculated step by step. With a starting estimate of the total air entrainment from Eq. 3 as ($Q_{air} = \beta\, q_w\, B$) (with an estimated value for Δp_0 of 2 to 8 kPa), the subpressure Δp_0 in the inlet area A_0 (Eq. 4) and Δp_B at the centerline of the spillway (Eq. 5) can be calculated. Starting at the spillway sidewall (inlet area A_0) the specific air entrainment $q_{air,1}$ for a width increment Δz can be calculated with the subpressure Δp_0. This yields the velocity $v_{air,1}$ at the end of the increment, and hence the subpressure at point 1 ($\Delta p_1 = \Delta p_B + \rho_{air} v_{air,1}^2/2$). This procedure is continued over all width increments up to the centerline ($z = B$), and it must be iterated until ($\sum q_{air,i} = Q_{air}$). In this way, the interaction of water and air flow is taken into account in calculating the total air entrainment.

6. CHANGES OF THE WATER FLOW DUE TO THE AERATION

The aeration of the high speed flow near the bottom leads to changes of the flow downstream of the aerators, which have to be considered in the design. These effects are:

- hydrodynamic forces in the region of the impact point of the jet,
- start of surface aeration (self aeration) at the location of the aerator,
- increase of the water depth due to the entrained air,
- waterspray at the surface,
- energy losses due to the entrainment process and the air transport,
- increase of the flow velocity along the jet length,
- increase of the flow velocity downstream of the aerator as a consequence of the reduction of the shear stress on the bottom due to the presence of air.

All these phenomena are discussed in *Koschitzky (1987, 1988)*. The most significant effect for the spillway and energy dissipator design (stilling basin, flip bucket) is the downstream flow acceleration due to the presence of air.

Downstream of the aerators, the flow reaches substantial air concentrations (up to 50%). The concentrations near the bottom are kept above 5% to 8 % for cavitation prevention by the proper spacing of the aerators. These air concentrations lead to a reduction of the friction coefficient and hence to an acceleration of the flow.

The wall shear stress is determined by the density of the air-water mixture $\rho_{air,w}$ near the bottom rather than by the water density ρ_w With the air concentration c_s near the bottom, the wall shear stress can be written as follows:

$$\tau_{s,air,w} = (\frac{\lambda_w}{8})\rho_{air,w} v_w^2 = (\frac{\lambda_w}{8})(\rho_w(1 - c_s))v_w^2 \qquad [6]$$

The ratio of the wall shear stress for the clear water flow to that of the air-water-mixture can then be written as:

$$\frac{\tau_{s,air,w}}{\tau_s} = (1 - c_s) \qquad [7]$$

which shows that an increase of the air concentration c_s leads to a decrease of the bottom friction and hence to an increase of the flow velocity.

For an estimate of this effect, the diagram of *Wood (1984)* in *Fig. 11* can be used. It shows that the friction coefficient ratio $\lambda_{w,air}/\lambda_w$ of the air-water-mixture to the clear water flow decreases drastically if the average air concentration in the flow reaches values higher than 20% to 30%. The addition of a scale for the air concentrations c_s near the bottom *(Fig. 11)*, which correspond to the cross-sectional averages of the equilibrium transport concentrations c, indicates clearly that c_s-values exceeding 2% to 5% already lead to substantial reductions of the wall friction coefficient.

Since for cavitation prevention the air concentrations c_s near the wall are usually kept well above 5 %, it is obvious that the flow in aerated spillways will experience considerably less frictional resistance and hence attain higher velocities than the unaerated flow. Prototype observations *(Minor, 1987)* confirm this in an impressive manner.

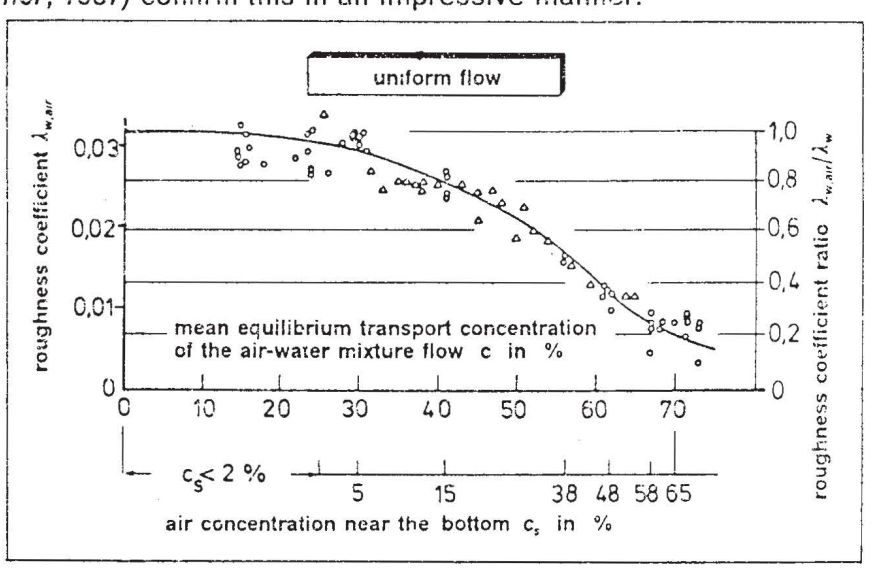

Fig. 11: *Influence of the mean air concentration on the friction coefficient in an air-water open channel flow (Wood, 1984) with corresponding values of the bottom air concentrations c_s (Koschitzky 1987)*

7. DESIGN PROCEDURE FOR SPILLWAYS WITH AERATORS

The design of a spillway with aerators involves a number of steps, as is shown in *Fig. 12*. Apart from the hydraulic design calculations for the water flow it requires the estimation of the cavitation danger, the design of the aerators and the consideration of the changes in the water flow due to the aeration. The design procedure indicated in *Fig. 12* is described in detail in *Koschitzky (1987)*. It provides a guidance towards a safe design and cavitation-free performance of spillways. Nevertheless, the confirmation of the design and the check on its performance requires specific and appropriate hydraulic model investigations.

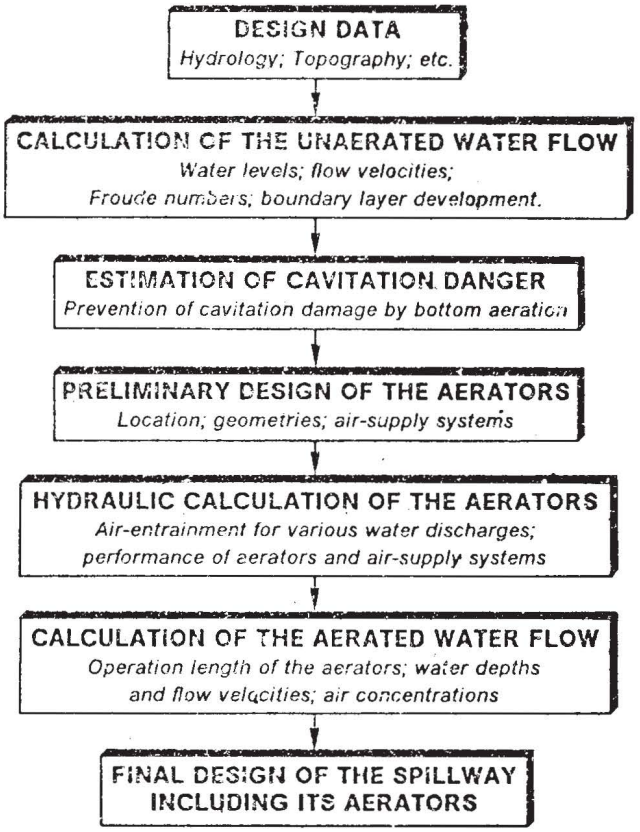

Fig. 12: *Design steps for spillways with aerators*

List of References

Kobus, H.: "Local Air Entrainment and Detrainment", IAHR Symposium on Scale Effects in Modelling Hydraulic Structures, Esslingen am Neckar, Germany, Sept. 1984, Paper 4.10, Proceedings, (Editor: H. Kobus)

Kobus, H.: "An Introduction to Air-Water Flows in Hydraulics", Mitteilungen Institut für Wasserbau, Universität Stuttgart, Germany, Heft 61, Oct. 1985

Koschitzky, H.-P.: "Dimensionierungskonzept für Sohlbelüfter in Schußrinnen zur Vermeidung von Kavitationsschäden", Mitteilungen Institut für Wasserbau, Universität Stuttgart, Germany, Heft 65, July 1987

Koschitzky, H.-P.: "Dimensionierung von Schußrinnenbelüftern", Wasserwirtschaft, Stuttgart, Germany, May 1988

Koschitzky, H.-P.; Westrich, B.; Kobus, H.: "Effects of Model Configuration, Flow Conditions and Scale in Modelling Spillway Aeration Grooves", IAHR Symposium on Scale Effects in Modelling Hydraulic Structres, Esslingen am Neckar, Germany, Sept. 1984, Paper 4.4, Proceedings (Editor: H. Kobus)

Koschitzky, H.-P.; Barczewski, B.: "Theoretische und experimentelle Vorstudien zur Frage des Lufteintrags und Lufttransports an Sohlbelüftern in Hochgeschwindigkeitsströmungen", Wissenschaftlicher Bericht HWV 089, Institut für Wasserbau, Universität Stuttgart, Germany, 1987

Low Heng Seng: "Model Studies of Clyde Dam Spillway Aerators", Research Report 86-6, Department of Civil Engineering, University of Canterbury Christchurch, New Zealand, March 1986

Minor, E.: "Erfahrungen mit Schußrinnenbelüftung", 7. Deutsches Talsperren-Symposium, March 1987, Wasserwirtschaft, Stuttgart, Germany, June 1987

Minor, E.: "Der Grundablass der Wasserkraftanlage Alicura in Argentinien", 7. Deutsches Talsperren-Symposium, March 1987, Wasserwirtschaft Stuttgart, Germany, June 1987

Pinto de S. N. L.; Neidert S. H.; Ota, J. J.: "Aeration at High Velocity Flows", Water Power & Dam Construction, London, U. K., Vol. 34, Feb/March, 1982

Pinto, N. L.: "Model Evaluation of Aerators in Shooting Flow", IAHR, Symposium on Scale Effects in Modelling Hydraulic Structures, Esslingen am Neckar, Germany, Sept. 1984, Paper 4.2, Proceedings, (Editor: H. Kobus)

Rutschmann, P.: "Transversale Druckverteilung unter Sprungstrahlen von Schußrinnenbelüftern - Folgen für den Lufteintrag", Wasserwirtschaft, Stuttgart, Germany, May 1987

Rutschmann, P.: "Belüftungseinbauten in Schußrinnen - Wirkungsweise, Formgebung und Berechnung von Schußrinnenbelüftern", Dissertation Nr. 8514, ETH-Zürich, Switzerland, 1988

Rutschmann, P.; Volkart, P.: "Spillway Chute Aeration - Interaction of Pumping Device and Supply System", Water Power & Dam Construction, London, U. K., Vol. 40, Jan. 1988

Tan, P.: "Model Studies of Aerators on Spillways", Research Report 84-6, Department of Civil Engineering, University of Canterbury Christchurch, New Zealand, Feb. 1984

Wood, I. R.: "Air Water Flows", 21st IAHR Congress, Melbourne, Australia, Aug. 1985

List of symbols

A_0	inlet area in the spillway side wall (m^2)	q_w	specific discharge (m^2/s)
B	spillway width (m)	q_{air}	specific air entrainment (m^2/s)
c	air concentration (-)	v	velocity (m/s)
c_s	air concentration near the bottom (-)	α	inclination angle of the spillway (°)
C1 C2 C3	coefficients (-)	β	specific air entrainment rate ($\beta = q_{air}/q_w$)
Fr	Froude number ($Fr = v_w/\sqrt{g\, y_w}$)	Δp	subpressure in the cavity below the nappe (kPa)
g	gravitational acceleration (m/s^2)	Θ	angle between ramp and spillway inclination (°)
l_s	length of the air duct system (m)	τ	wall shear stress (MN/m^2)
Q_w	water discharge (m^3/s)	ζ	loss coefficient (-)
Q_{air}	total air entrainment (m^3/s)	λ	friction coefficient due to roughness (-)
		ρ	density (kg/m^3)